APPLICATIONS OF ASTEC CODE IN RELATION WITH HYDROGEN GENERATION ON A GENERIC CANDU 6 REACTOR

GABRIELA RADU
Institute for Nuclear Research (RATEN ICN) Piteşti, Romania
e-mail: gabriela.radu@nuclear.ro

Abstract

Under severe accident conditions in nuclear power plants with water cooled reactors, large amounts of hydrogen can be generated and released into the reactor containments. Hydrogen can be produced from oxidation of the metallic components of the core and molten core-concrete interaction (MCCI) after failure of the reactor vessel and relocation of the corium consisting of the molten reactor core and internal structures to the reactor cavity. A large amount of carbon monoxide may also be produced during MCCI in addition to hydrogen and other gases. This could potentially lead to the formation of flammable mixtures of gases in reactor containments. An accidental combustion of these mixtures could lead to pressure and temperature levels that may jeopardize the containment integrity. Hydrogen combustion can cause containment building failure by dynamic pressure and impulse loads, missile generation, and equipment failure due to temperature or pressure effects. The present paper aims to present the ASTEC modelling of the severe core damage phase and molten core-concrete interaction in the reactor vault for a CANDU6 reactor during a loss of coolant accident focusing on hydrogen and carbon monoxide generation.

Keywords: *ASTEC, CANDU, Hydrogen, Severe accident*

Introduction

The core of the CANDU6 pressurized heavy water reactor consists in 380 horizontal fuel channels submerged in a large volume of sub cooled heavy water moderator in a stainless steel horizontal cylindrical vessel (called the calandria). The calandria vessel is located inside a steel-lined concrete reactor vault filled with light water. Each fuel channel consists of a Zr-2.5wt%Nb pressure tube surrounded by a Zircaloy-2 calandria tube with a carbon dioxide gap in between. Each pressure tube contains twelve 0.5 m long fuel bundles each consisting of 37 Zircaloy-4 clad fuel elements containing uranium dioxide (UO_2) pellets. The heat produced in the fuel pellets is removed by heavy water coolant flowing through the fuel channels at high pressure and temperature. The coolant is circulated through the pressure tubes by the primary heat transport system pumps via the inlet and outlet feeder pipes connecting the respective inlet and outlet headers. The heat generated in the reactor is carried by the reactor coolant to the steam generators, where it is transferred to light water to produce steam to drive the turbine. The total core fission and decay heat at normal operation conditions is 2156 MW. The 380 fuel channels are arranged in 22 rows and 22 columns. The 22 vertical columns of fuel channels are divided into 2 loops symmetric about the vertical axis. Each loop consists in two core passes of 95 channels each.

For a pressurized heavy water reactor (PHWR), there are two classes of accidents that result in damage to the reactor core, depending on the availability of the moderator heat sink [1]: (1) limited core damage accidents (LCDAs) where the core geometry is preserved and (2) severe core damage accidents (SCDAs) where the core geometry is lost. The LCDAs can involve single or multiple channels. In both cases, the presence of moderator heat sink prevents failure of the fuel channels and core degradation. The SCDAs are severe accidents. SCDA initiates as a LCDA, but the moderator cooling system is unavailable and there is no moderator make-up. In this case, the moderator would boil off and the uncovered fuel channels heat up. The channels would gradually sag during the heat up and disassemble on the adjacent channels located below. A suspended coarse debris bed is thus formed, which move downward with the falling moderator level. When the hot suspended debris and sagged channels exceed the load supportable by the cool intact channels, most of the core collapses into the water pool at the bottom of the calandria vessel. A hot dry debris bed would form on the bottom of calandria vessel after the remaining moderator evaporation due to the decay heat from the core debris. This debris bed transfers heat to the calandria vault water which acts as the ultimate heat sink.

In this paper the version ASTECv2.1.1.6 has been used to simulate the in-vessel core degradation, from the start of core uncover, for a generic CANDU 6 reactor following a large break loss of coolant accident with simultaneous loss of power. Also, the reactor vessel failure and the corium-concrete interaction in the reactor vault are simulated. The aim of the paper is to estimate the hydrogen and carbon monoxide generated during the accident.

Computer code

ASTEC (Accident Source Term Evaluation Code) [2] is a severe accident integral code, jointly developed by the French Institut de Radioprotection et de Sûreté Nucléaire (IRSN) and the German Gesellschaft für Anlagen und Reaktorsicherheit mbH (GRS) between 1996 and 2015 and by IRSN alone afterwards, for simulating complete severe accident sequences in water-cooled reactors from the initiating event up to a possible release of fission products out of the containment, including the behaviour of safety systems and procedures used in Severe Accident Management (SAM). The ASTEC scope of applications covers most of the severe accident phenomena, except steam explosion and mechanical response of the containment. The code structure is modular, each of its modules simulating a reactor zone or a set of physical phenomena.

Since 2004, ASTEC has gradually become the European reference severe accident code for water-cooled nuclear reactors by capitalizing the knowledge gained largely within the SARNET European Network of Excellence (FP6 and FP7) [3, 4], in OECD and ISTP ((International Source Term Programme) projects. Concerning the ASTEC applicability to PHWR plant type, most of the ASTECv2.0 modules were considered suitable enough to support analyses addressing such plant while the ICARE module, which describes in-vessel core degradation phenomena, was unable to represent the core geometry for PHWR reactor type. Specific developments [5-7] have been made in ASTECv2.1 to make it possible to describe both axi-symmetrical cores (such as PWR) and multi-channels cores (as in case of existing BWR and CANDU reactors). Also, ASTECv2.1 is able to address fluid flows in horizontal cores, while it was not the case of the former v2.0 version [7].

The code modules used for this paper are CESAR, ICARE and MEDICIS.

The CESAR module [2] describes the primary and secondary thermal-hydraulics during a nuclear reactor accident. The CESAR thermal-hydraulics modelling is based on a 1D two-fluid 5-equation approach. The 5-equation model involves four mass and energy conservation equations for the liquid and gas phases and one momentum conservation equation for the two-phase mixture. The mechanical non-equilibrium between phases is simulated by a set of drift correlations. Thermal non-equilibrium is described with interfacial heat transfer models. CESAR of ASTEC v2.1 enables to include in the simulation up to 5 non-condensable gases. The finite volume approach is used to discretize in space the considered geometry.

The ICARE module [2] describes the in-vessel core degradation phenomena during a severe accident of a reactor. It computes the behaviour of in-vessel structures, the formation and the evolution of liquid and solid mixtures and chemical reactions between materials.

The MEDICIS module [2, 8] simulates MCCI (Molten-Core-Concrete Interaction) using lumped parameters 0D approach with averaged melt/crust layers. The code assumes either well-mixed oxide/metal pool configuration or possible pool stratification into separate oxide and metal layers. In both cases, the crust that can grow up at the upper interface of the corium pool may be described in detail. Also, if there is a water pool above the corium, a debris bed can be formed due to the melt eruption mechanism. Starting with a homogeneous or a stratified configuration, the pool configuration may evolve versus time. It describes concrete ablation, corium oxidation and release of non-condensable gases into the containment. Most convective heat transfer correlations available in literature for the corium/concrete interface and the interface between corium layers are included. Its structure is flexible enough to allow optional models and correlations or an easy implementation of new models. Regarding the concrete cavity of the reactor pit, its shape can be axi-symmetric. MEDICIS uses a robust cavity erosion algorithm including the possibility to represent a multi-layered concrete base mat. The module is interfaced with the general physics-chemistry package MDB (Material Data Bank) of ASTEC for element speciation in a mixture, thermodynamic data and thermo-physical properties. MEDICIS contains models for corium-quenching, ex-vessel corium pool release of concrete aerosols and fission products release during MCCI, etc.

Accident scenario

The scenario considered is a large break loss-of-coolant accident with simultaneous loss of Class III and IV power. In this case, the moderator cooling and shield cooling are unavailable. Also, the emergency core cooling, the main and auxiliary feed water are unavailable.

When the severe core damage occurs, four phases of accident progression are expected. First phase covers the accident initiation until the complete voiding of fuel channels and phase 2, from the complete voiding of the fuel channels to core collapse. As a result of the loss of the primary coolant, in the early phase of the accident, the fuel, sheath and pressure tube temperatures start rising. During high temperature transient, the pressure tube (PT) deforms and contacts the calandria tube (CT) due to sagging/ballooning. This causes heat removal through PT and CT to moderator. The deformation can arrest for a time the pressure tube temperature rise in presence of moderator surrounding the calandria tube. During the second phase of the accident, the moderator temperature increases because of the loss of moderator cooling and the heat transfer from the core. The moderator starts to boils-off and the uncovered fuel channels heat up and fail. This phase terminates with the complete disassembly of the reactor core and its collapse into the bottom of the calandria vessel. After the core collapse to the calandria vessel failure, phase 3 includes phenomena regarding the heat transfer from the core debris to the moderator, the moderator boil-off, heat up of the calandria, heat transfer from the calandria external surface to the vault water and the vault water boil-off. Phase 4 of the accident starts from the calandria vessel failure to the calandria vault failure due to the ablation. During this phase, the water remaining in the reactor vault is evaporated and the molten core relocated onto the vault floor interacts with the concrete inside the reactor vault.

ASTEC modelling

The CESAR and ICARE modules are used to simulate the severe core damage and the behaviour of the debris bed and of the vessel during the phase 2, and 3. In phase 4, after the molten is relocated into the reactor vault, the corium-concrete interaction is modelled with the MEDICIS module. The first phase of the accident progression is not presented in this paper. The second phase is assumed to start at 500 s after the initiating event. Other initial conditions used in calculation were, as follows: moderator temperature and pressure of 65 °C and 123 kPa(a), respectively; moderator mass of 227000 kg; fuel and cladding temperature of 1500 K; pressure tube temperature of 1400 K; calandria tube temperature of 348 K.

CESAR modeling

In the second phase, only the moderator volume is modelled to evaluate the moderator boil off. The fuel channels are assumed voided. The calandria vessel containing the moderator is discretized into ten (10) vertical volumes (Fig. 1). The top moderator volume is connected to four over pressure relief lines with rupture discs which open when the moderator pressure exceeds 238 kPa (a). This volume is also connected to a release valve which opens at 30 kPa (g). Each moderator volume, from V_modr2 to V_modr9, is associated with a wall which represents the calandria tubes at the respective volume level. A fictitious wall is also used to represent the channel walls which collapse to the calandria bottom.

After the core collapse, the phase 3 of accident is assumed to begin with entire core in form of debris bed on the bottom of the vessel. The vault water and end shield cooling water are modelled with the help of CESAR volumes (volumes with swollen water level). The vault connection to atmosphere and the end shield connection to atmosphere through rupture discs are modelled using CONNECTI structures. These rupture discs open at 68.9 kPa (g). The vault walls are modelled as a single wall component in CESAR. Also, various structures connected to the end shield are modelled as CESAR walls. The heat transfer from the external surface of the calandria vessel to the vault water is modelled by using sensors, events and boundary conditions.

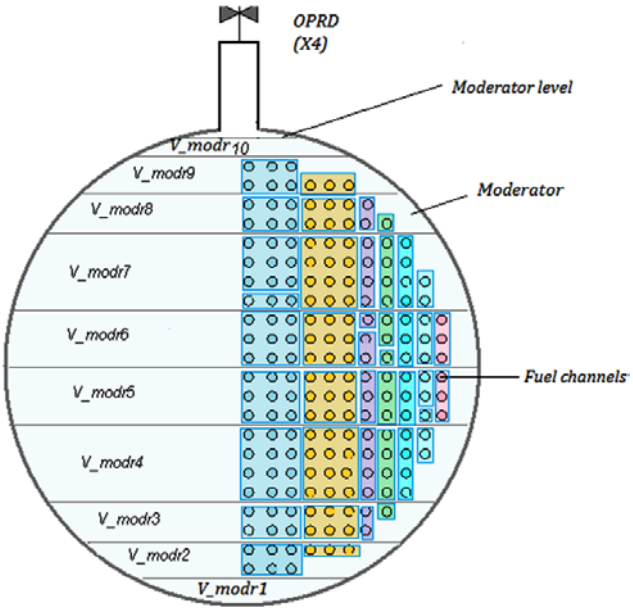


Fig. 1. Reactor core and moderator nodalization

ICARE modelling

In phase 2, the core model comprises 42 core channels (one half of the reactor core) heaving different power and elevation within the calandria vessel (as seen in Fig. 1). Each channel comprises fuel bundle, pressure tube (PT) and calandria tube (CT). The core is discretized into 12 axial meshes. Channel components are defined as macro-component structures.

The modelling includes a single representative fuel element for 37 identical assumed elements (one macro-component for fuel and one macro-component for fuel cladding with the weight 37). Fuel elements in the bundle are assumed arranged uniformly in a triangular array. The moderator is being modelled in CESAR module.

Two fluid channels are defined, one inside the pressure tube and the other outside the calandria tube (see Fig. 2). Both the channels are fully voided. The steam flows have been imposed at the inlet of these channels. The channel outside the calandria tube is only used to facilitate the oxidation of the calandria tube at external surface.

The power distribution for a CANDU 6 reactor is shown in Fig. 3 a) [9]. The core (a loop) is divided into 42 zones and the average power obtained for each zone is shown in Fig. 3 b). Only one channel in each zone is considered in the modelling, the total power of the core being around 424.6MW.

Channel disassembly is assumed to occur if the average temperature of the channel (pressure tube and calandria tube) exceeds 1473 K [1]. The complete collapse of a vertical column of core channels occurs if top 7 rows of channels (Figs. 1 and 3) have disassembled [1].

At the outer periphery of the core where 7 rows are not available, a criterion based on the zircaloy melting temperature is used for disassembly. Once a channel has relocated to the bottom of the vessel, the heat emitted from the outer surface of the channel calandria tube is added to the moderator volume at the lower level through the fictitious wall defined in CESAR module. On the outer surface of the calandria tubes, the heat transfer coefficient as a function of temperature is imposed to simulate the pool boiling behaviour of the moderator. The heat is transferred to the moderator volume through the calandria tube walls modelled in the CESAR module.

Zircaloy calandria tubes exposed to steam are assumed to be always oxidized by steam at their outer surface, whereas at the inner surface oxidation occurs when they have cracked (at 1473 K). The oxidation of the pressure tube and fuel cladding could occur after the channel disassembly. The parabolic correlation used for Zircaloy oxidation by steam is the ″BEST-FIT″ correlation for Zircaloy-4 material (elaborated for ICARE) [10, 11]. This correlation includes three temperature regions: below 1798 K, a transition temperature region from low to high temperatures, and above 1900 K.

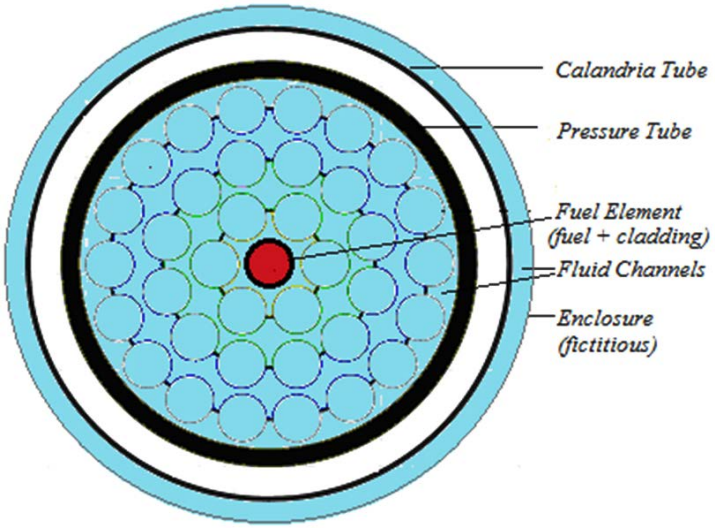
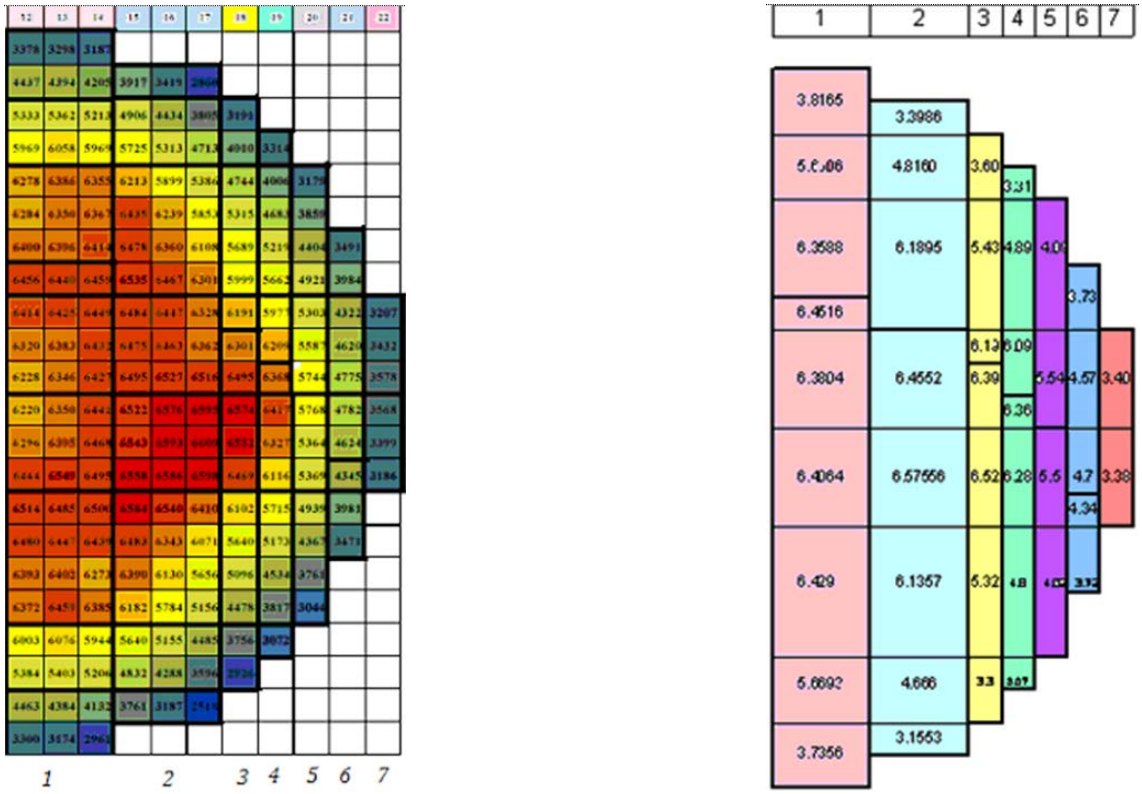


Fig. 2. View of ICARE radial modelling for a representative channel
(only one fuel element is modelled with an associated weight 37)



a) Power distribution for half a core of CANDU6, [kW] b) Average power distribution of the 42 zones, [MW]

Fig. 3. Power distribution

For the third phase of the accident progression, which begins with the entire core collapsed on the bottom of calandria vessel and submerged in the remaining moderator, the ICARE modelling includes the calandria vessel and internals (the channels relocated in form of debris). The initial level of moderator present within the calandria is defined as FLUID [10] component with definition of initial temperature, void fraction and level.

In the ICARE module, the description of the core area is separated from the lower plenum area which is described by a single dedicated mesh. In this mesh, the physical phenomena are described by dedicated physical models different from those used for the core area.

For PHWR, the reactor vessel and the lower plenum are a single entity, namely the calandria. Calandria is modelled by the model STRU LOWERPLE [10]. This structure enables to represent the vessel as well as the materials relocated inside (debris bed). A debris layer has been defined at the lower position within the lower plenum structure. The CANDU 6 core has an inventory of 98815 kg uranium dioxide and 38647 kg Zircaloy [12]. The mass of the debris bed layer is 138536 kg, the layer composition is UO2/Zr/ZrO2 with the mass fractions of materials of 0.713/0.257/0.03 and the porosity is assumed to be 0.4. Also, three end shield layers have been defined. End shield components are used for closing the calandria from both ends. End shield consists of layers of stainless steel tube sheets and carbon steel balls and light water. The end shield cooling water has been considered in CESAR. The physical phenomena modelled are the conductive and convective heat exchanges and the mass exchanges within the lower plenum, the radiative heat exchanges within the calandria, the movement of debris and magma within the lower plenum, decanting and phase separation inside/ between corium layers. No oxidation of the debris is modelled within the lower plenum.

The calandria vessel failure is considered based on maximum molten fraction of the vessel wall.

MEDICIS modelling

The reactor vault is a rectangular reinforced concrete compartment lined inside with a thin layer of steel, filled with light water (about $5.0 \cdot 10^5$ kg [13]) that contains and supports the whole reactor assembly. Data for the reactor geometry, material composition and initial conditions used in the MEDICIS calculation are listed below:

- It was assumed an axi-symmetric initial vault shape, cylindrical geometry with the radius of 4.12 m (equivalent radius deduced from the floor area) and the height of 13.4 m [13].
- The thickness of the lateral reactor vault walls is assumed to be 2 m (for present paper).
- Thickness of the vault floor: 2.4 m
- Initial corium mass: 148465 kg
- Initial corium temperature: 2200 K.
- Initial corium composition: (66.5/2.8/23.9/6.8 wt% UO_2/ZrO_2/Zr/stainless steel); it was assumed that 10% of the mass of the stainless steel vessel walls [13] is contained in the initial corium pool.
- Concrete characteristics: reinforced siliceous concrete.

It was assumed an initial vault shape without round corner. The initial number of nodes is 180. The cavity is meshed from the central node to the last one that corresponds to top of the vault. The erosion is allowed in any direction. Concerning the concrete simulated, a siliceous concrete with 64.5% O_2Si, 18% CaO, 3.7% Al_2O_3, 4% H_2O, 9.8% CO_2 weight fractions was considered [14, 15] for present paper. A mass fraction of iron bars embedded in the concrete of 6.5% was taken into account in MCCI calculations [14]. The ablation temperature of this concrete was assumed to be equal to 1550K, its ablation enthalpy variation was set to $1.91 \cdot 10^6$ J/kg [15], and its density was chosen near 2400 kg/m^3.

Main modelling assumptions and values of key physical parameters used in the MEDICIS calculation are presented herein after.

The corium pool configuration was assumed homogeneous (a mixed oxide/metal layer) with an upper crust at the corium-water-pool (atmosphere) interface. The crust that can grow up at the upper corium pool interface is represented by a second layer, for which temperature, composition, and species fluxes coming in and going out are calculated. Also, a debris-bed can be formed at the top surface of the corium pool due to the melt eruption mechanism. This accumulation of corium particles forms a layer above the detailed upper crust which is supposed to remain at water temperature. In case of dry-out due to reduction of water inventory, the dry-out debris will re-melt and incorporate in the upper crust.

The corium pool/concrete interface structure model determines the thermal resistance and thus the local heat flux from the corium pool to the concrete. Standard modelling assumptions in MEDICIS were used for this calculation. The interface model used assumes the existence of a mushy zone at the interface between the liquid pool and the concrete consisting of a convective zone and a conductive zone. Heat is transported by gas bubbling across this pool mushy zone and then, as the solid fraction is high enough, by conduction to the concrete ablation interfaces [16]. The temperature of the boundary between pool conductive and convective zones is the solidification temperature. A slag layer is also assumed to exist between the concrete and the pool. In present paper, the value of the convective heat transfer coefficient in the slag layer along the concrete interface is assumed constant and equal to 1000 W/m^2/K [16-18]. The pool solidification temperature is evaluated from solidus and liquidus temperature of the corium-concrete mixture as a function of time using the below given formula [18]:

$$T_{solidif} = \gamma \cdot T_{solidus} + (1-\gamma) \cdot T_{liquidus} \qquad (1)$$

where the interpolation parameter, $\gamma = 0.3$, in present paper.

The heat exchange coefficient by convection between the corium layer and the concrete was evaluated from a correlation derived from the BALI experiments [19]. The value of the melt eruption coefficient (Spalding's model) was 0.08 and the permeability of the upper crust was set to 10^{-10} m^2. The corium properties were determined from the Material Data Bank (MDB) library of ASTEC.

The MEDICIS calculations were pursued until axial or radial melt-through.

ASTEC simulation results

The results of the ICARE-CESAR simulation of the in-vessel core degradation during the phases 2 and 3 of the accident progression are presented in Figs. 4-21. Tables 1 and 2 summarize the timing of some events predicted by the code.

Table 1 Sequence of some events for phase 2

Time [h]	Event
0	Start of phase 2
1.3	First channel row is uncovered
1.7	Beginning of core disassembly
2.8	Beginning of core collapse
7	Entire core collapsed onto the calandria vessel bottom

Table 2 Sequence of some events for phase 3

Time [h]	Event
0	Start of phase 3
3	Water is depleted inside calandria vessel
4	Reactor vault/end shield rupture discs open
34.7	Water level in the reactor vault falls below calandria vessel bottom
40.5	Calandria vessel failed

During the second phase, the moderator temperature starts to rise and ultimately it starts to boil off and uncover the upper fuel channels. The uncovered fuel channels heat up, deform and disassemble into core debris. This phase terminates with reactor core collapse in the calandria. The third phase of the severe accident begins with the entire reactor core relocated on the bottom of the calandria vessel and extends up to the failure of the vessel.

The severe core damage and the subsequent relocation of the core material are closely connected with the moderator behaviour in the reactor vessel. The moderator temperature and pressure in the calandria vessel increase due to the lack of moderator cooling and the heat transfer from the core channels to the water. When the pressure inside the calandria reaches the set point of the rupture discs, they fail, resulting in moderator expulsion through the relief ducts. The moderator continues to discharge into the containment atmosphere, resulting in a gradual decrease of the water level in the calandria vessel. Figs. 4 and 5 show the moderator level and moderator mass, respectively.

The water and steam mass flow rates through a rupture disc are shown in Figs. 6 and 7, respectively. The heat transferred from the calandria tubes to the moderator is shown in Fig.8 and the moderator void fraction is presented in Fig.9.

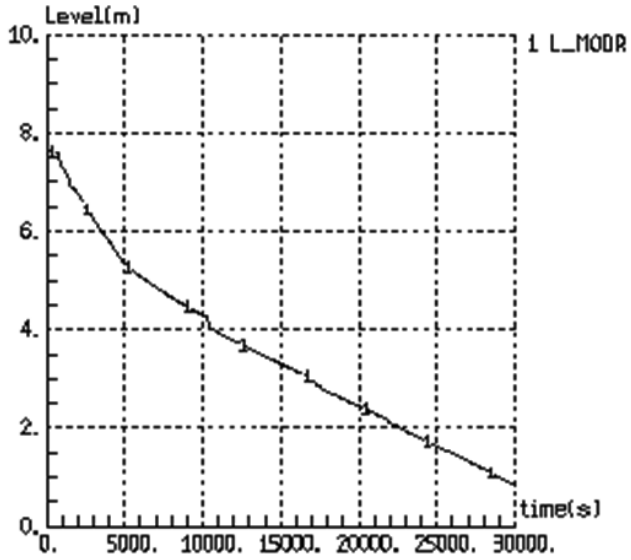


Fig. 4. Moderator level

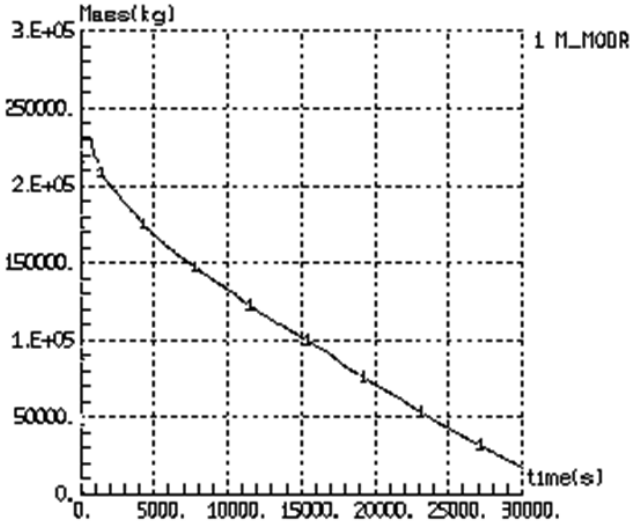


Fig. 5. Moderator mass

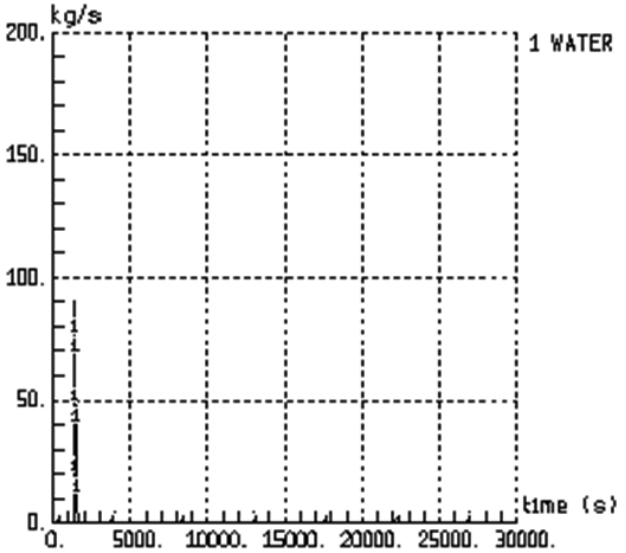


Fig. 6. Water mass flow through connection OPRD1

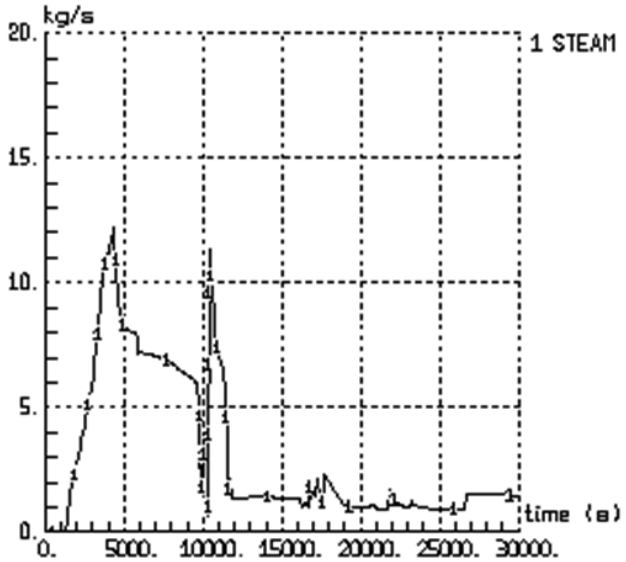


Fig. 7. Steam mass flow through connection OPRD1

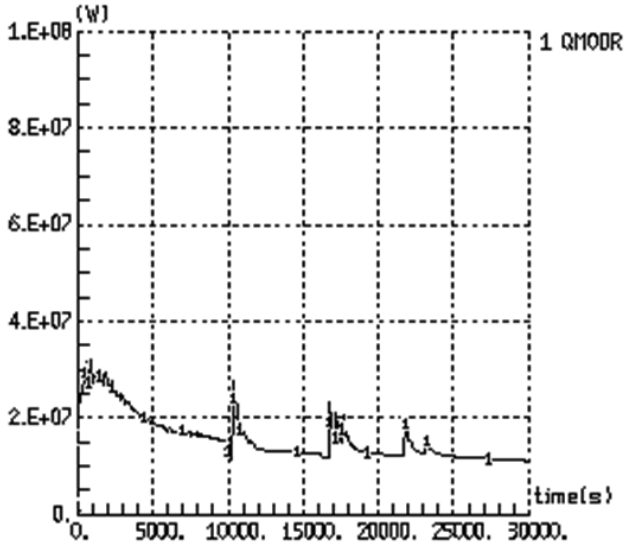


Fig. 8. Heat transfer rate to moderator

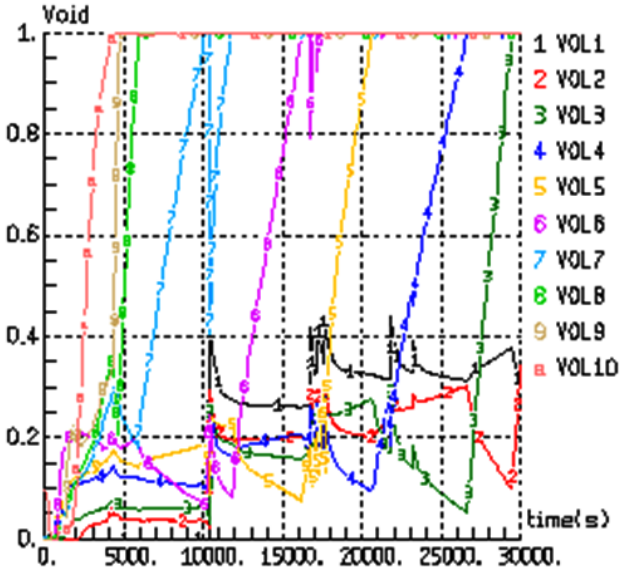


Fig. 9. Moderator void fraction

The uncovering of the first row of channels occurs at around 1.3 h from the start of second phase. The exposed channels get heated up due to decay heat and heat generated due to metal-water reaction. The temperatures of the fuel, sheath, pressure tube and calandria tube for the top three channels on column 1 (see Fig. 3 b)) are shown in Figs. 10-13. For these channels, Fig. 14 shows the average temperature of the calandria tube and pressure tube. When the average temperature of the pressure tube and calandria tube reaches 1473 K it is considered that the channel fails and dislocates from its position and rests on the channel underneath. The disassembly of the upper channels begins at about 1.7 h from the beginning of second phase of the accident. At around 2.8 h, the reactor core collapse begins and at nearly 7 h the entire core is relocated to the bottom of the calandria vessel and immersed in the remaining moderator (Figs. 15 and 16). Due to Zircaloy oxidation reaction, hydrogen is generated (Figs. 17 and 18). The Hydrogen amount generated mainly from the calandria tubes oxidation (inside and outside surface) is ~110 kg. The maximum hydrogen generation rate during this phase is about 0.05 kg/s. Only a very small amount of hydrogen is generated from the pressure tubes and the fuel sheaths.

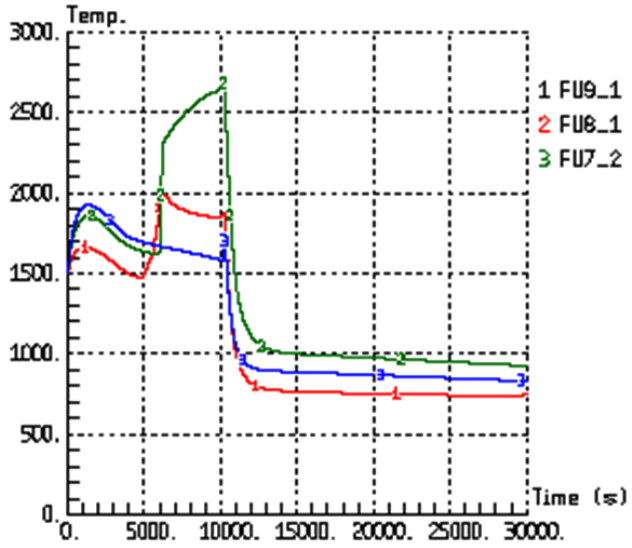


Fig. 10. Fuel temperature

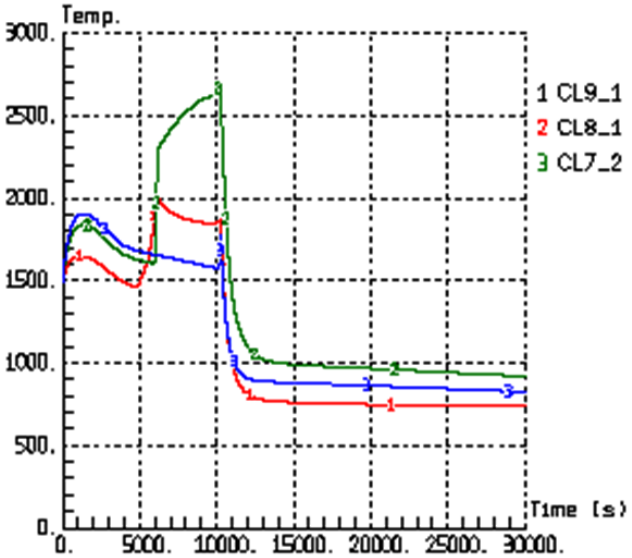


Fig. 11. Cladding temperature

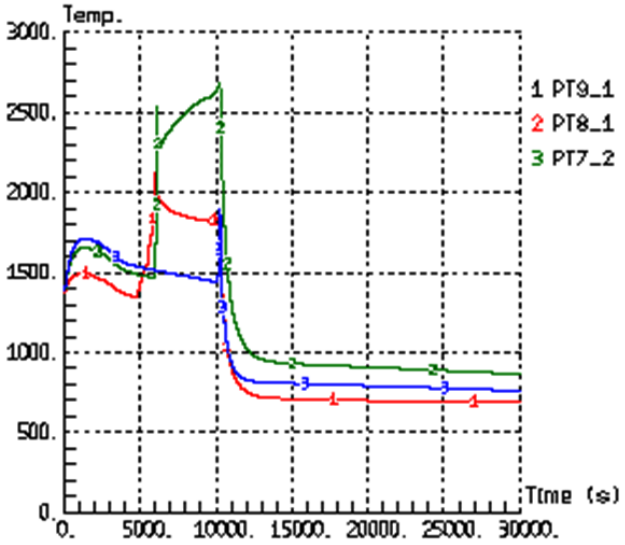


Fig. 12. Pressure tube temperature

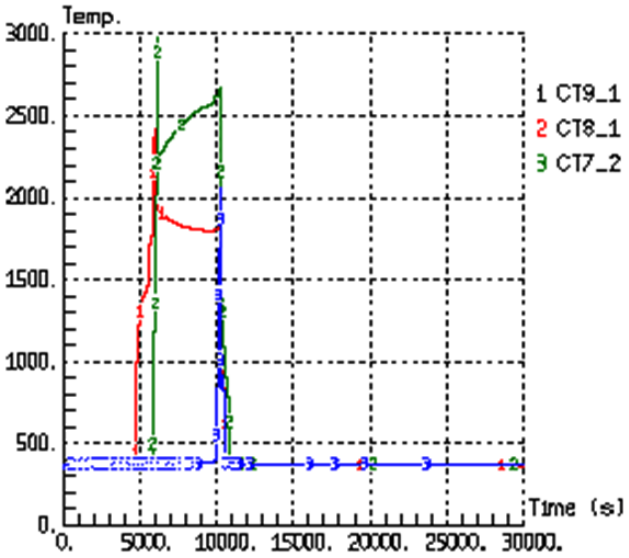


Fig. 13. Calandria tube temperature

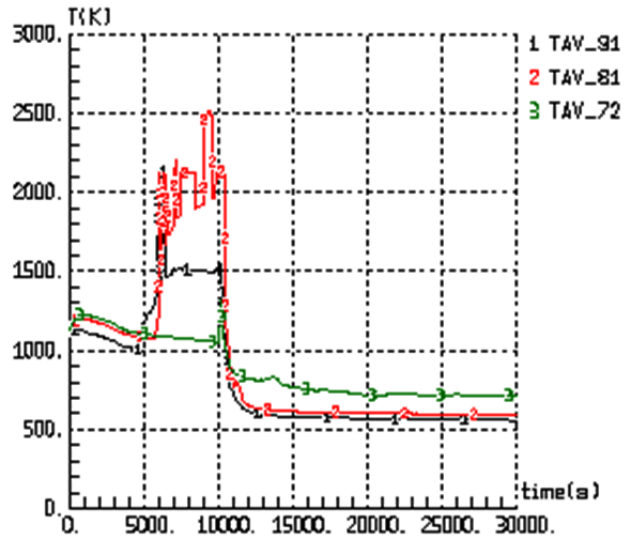


Fig. 14. Average temperature of the pressure tube and the calandria tube in the column 1

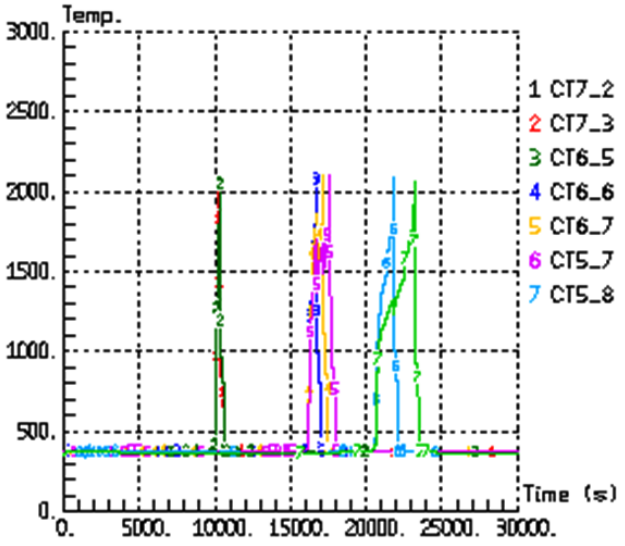


Fig. 15. Temperature of calandria tube in the seventh fuel channel, in each column

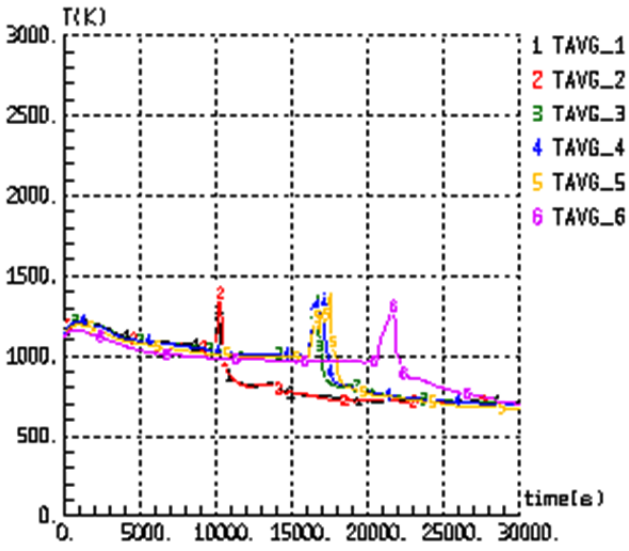


Fig. 16. Average temperature of calandria tube/ pressure tube

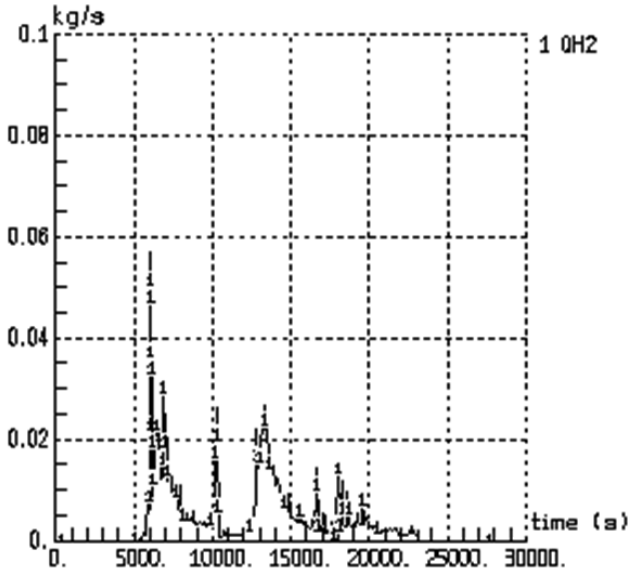


Fig. 17. Hydrogen mass flow rate evolution (from CTs)

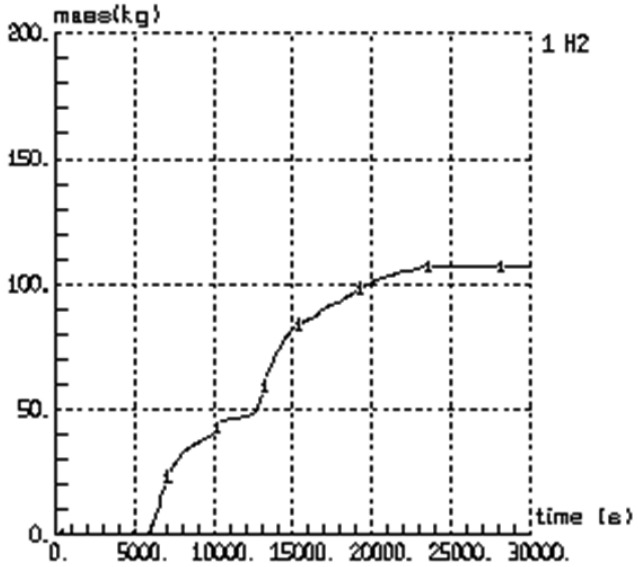


Fig. 18. Hydrogen mass from CTs

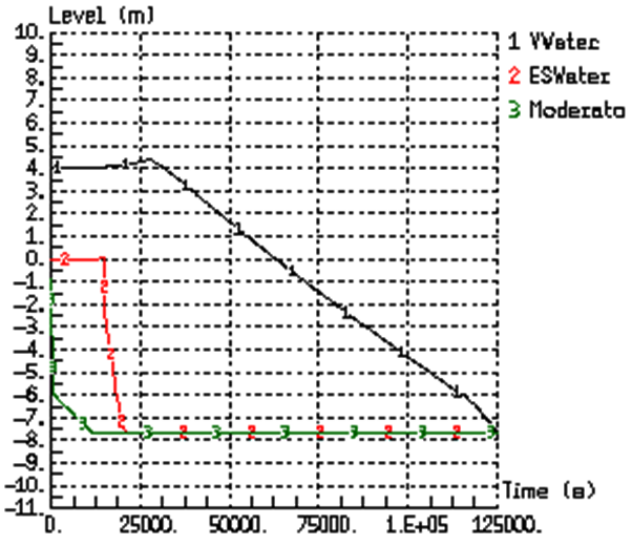


Fig. 19. Water level in the vault, end shields and calandria

After the complete collapse of the reactor core, all the channels are at the bottom of the calandria and submerged in moderator. At the time of the core collapse, the moderator level is 1.89 m. The core debris continuously gets cooled by boil off of moderator. The water in the calandria vessel is depleted at about 3 h from the beginning of the third phase (about 10 h after the initiating event). After boil off of the moderator, the temperature of the debris continuously increases. Melting occurs after about 40 h from the beginning of the third phase.

The water in the reactor vault acts as a heat sink and cools the walls of the calandria vessel, maintaining its integrity. The temperature and pressure in the reactor vault and end shields increase gradually due to the lack of shield cooling and heat transfer from the core debris to the shield water. At ~ 4 h from the beginning of the third phase of the accident, the vault/end shields rupture discs open when the pressure difference exceeds 69 kPa. The vault water continuously gets heated and evaporated resulting in a gradual water level decrease. The water level in the reactor vault falls below the bottom of the calandria vessel at nearly 34.7 h from the beginning of the third phase. Fig. 19 shows the evolution versus time of the water level in the reactor vault, end shields and calandria.

The reactor vessel fails by fusion (when the maximum liquid fraction of the wall is reached) at approximately 40.5 h from the beginning of the third phase.

Figs. 20 and 21 show the corium mass and corium temperature during the phase 3. No hydrogen generation was calculated during this phase. When the calandria vessel fails, all corium falls into the reactor vault. After the depletion of the water in the reactor vault, the corium reacts with the concrete walls of the vault.

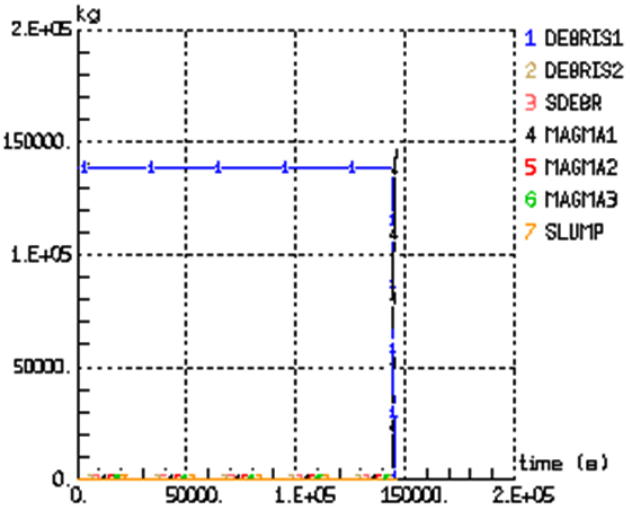


Fig. 20. Corium mass in the lower plenum

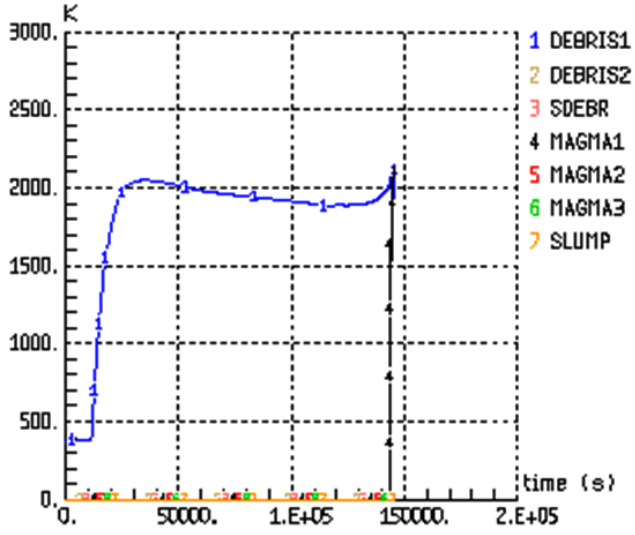


Fig. 21. Corium temperature in the lower plenum

The results of the ASTEC/MEDICIS calculation are presented in Figs. 22 - 25.

The uniform distribution of the heat transfer coefficient along all the pool/concrete interfaces leads to spatially nearly uniform ablation depths. Fig. 22 shows the erosion of the reactor vault concrete walls in the radial (Rmax) and axial (Zmin) directions. The lateral melt-through occurs at around 141 h from the beginning of phase 4, the thickness of the lateral walls being considered 2m in this paper. Fig. 23 illustrates the final shape of the ablated vault during the interaction between the molten corium and the concrete. At the end of the calculations, the total mass of the ablated concrete is about 690000 kg and the maximal vertical ablation depth is about 2.11 m. The final thickness of the upper crust is near of 0.24 m and the thickness of the oxide layer 2.18 m.

The water vapour and carbon dioxide that are released from the concrete during the corium–concrete interaction react with the metals in the melt and produce H_2 and CO. Zirconium is oxidized first, and silicon, chromium, nickel and iron follow in this order. Fig. 24 gives the mass flow rates of gases produced by MCCI and released in the reactor vault. The mass of hydrogen generated during the corium-concrete interaction in the reactor vault is about 870 kg at the melt-through time, and the mass of carbon monoxide is near 21100 kg (Fig. 25). At the end of calculation, the amounts of CO_2 and H_2O released into the vault are about 30400 kg and 17800 kg, respectively.

The maximum generation rates are about 0.0146 kg/s in the early stage of ex-vessel phase and about 0.00092 kg/s later in the accident for the hydrogen (Fig. 24), and about 0.206 kg/s in the early stage of MCCI and 0.03 kg/s in the late stage for the carbon monoxide.

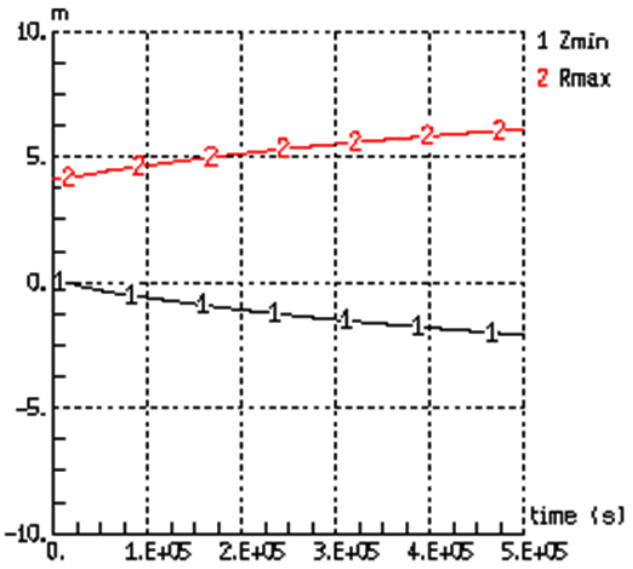


Fig. 22. Lateral and axial ablation kinetics

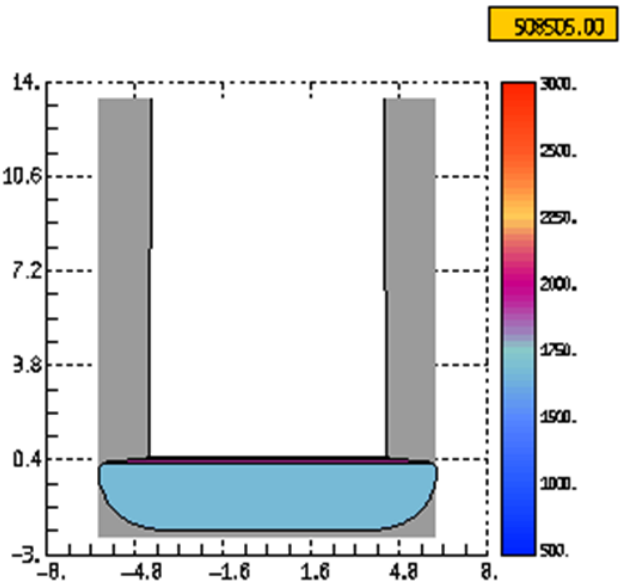


Fig. 23. Final shape of the reactor vault

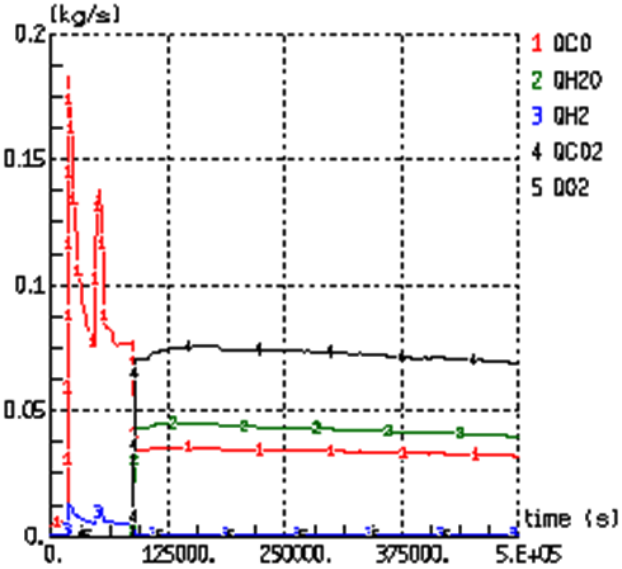


Fig. 24. Gas mass flow rate during MCCI

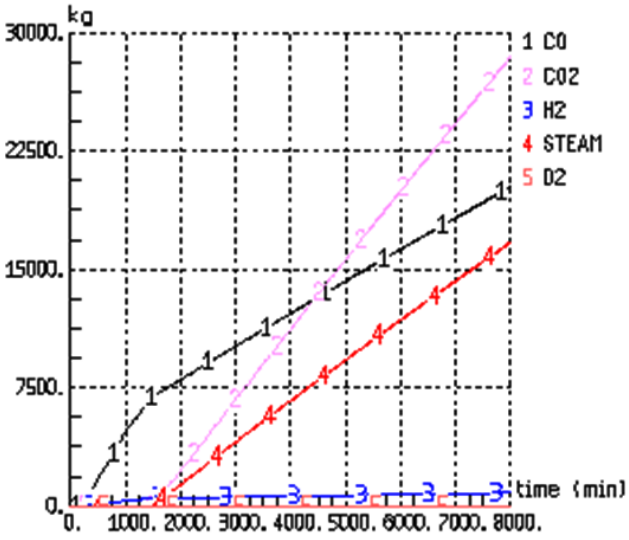


Fig. 25. Corium concrete gas production mass

Conclusions

In present paper, ASTECv2.1.1.6 version was used to simulate the severe core damage phase for a generic CANDU 6 reactor following a large break loss of coolant accident with simultaneous loss of power with the aim to estimate hydrogen production. Also, the terminal debris bed behaviour, the reactor vessel failure and the molten core-concrete interaction within the reactor vault were simulated.

This paper demonstrates the capability of ASTEC code to simulate the in-vessel core degradation for CANDU 6 reactors. One of the code limitations refers to the simulation of the debris oxidation.

The hydrogen generated in-vessel includes the hydrogen produced in the intact fuel channels and suspended disassembled channels. Major contribution to the hydrogen production occurs after the pressure and calandria tubes fail due to excessive heating of the fuel channels without cooling. No hydrogen generation in the terminal debris bed located on the calandria vessel bottom was calculated. Large quantities of hydrogen and carbon monoxide are generated in the reactor vault due to the molten core - concrete interaction. The hydrogen total mass and the hydrogen production rate are the most important parameters influencing the development of a flame acceleration combustion process which could jeopardize the containment integrity. The total amount of hydrogen generated in-vessel and ex-vessel depends on the oxidation models used in the fuel channels, core disassembly, debris cooling and MCCI stages.

An important parameter is the surface area exposed to steam in the intact and disassembled fuel channels. Also, the concrete composition is an important parameter that determines the erosion progression and gas release during corium-concrete interaction.

References

[1] International Atomic Energy Agency (2008) ″Analysis of Severe Accidents in Pressurized Heavy Water Reactors″, *IAEA-TECDOC-1594*, IAEA, Vienna, Austria

[2] Chatelard, P., Reinke, N., Arndt, S., Belon, S., Cantrel, L., Carenini, L., Chevalier-Jabet, K., Cousin, F., Eckel, J., Jacq, F., Marchetto, C., Mun, C., Piar, L. (2014) ″ASTEC V2 severe accident integral code main features, current V2.0 modelling status, perspectives″, *Nuclear Engineering and Design*, Vol. 272, pp.119-135

[3] Micaelli, J.C., Van Dorsselaere, J.P., Chaumont, B. (2005) ″SARNET: a European Cooperative effort on LRW severe accident research″, Proc. of European Nuclear Conference, Versailles, France

[4] Van Dorsselaere, J.P., Auvinen, A., Beraha, D., Chatelard, P., Journeau, C., Kljenak, I., Sehgal, B.R., Tromm, W., Zeyen, R. (2010) ″Status of SARNET network on severe accidents″, Proc. of Int. Congress on Advances in Nuclear Power Plants (ICAPP'10), San Diego, USA

[5] Majumdar, P., Chatterjee, B., Lele, H.G., Guillard, G., Fichot, F. (2014) ″ASTEC adaptation for PHWR limited core damage accident analysis″, *Nuclear Engineering and Design*, Vol. 272, pp.273-286

[6] Nowack, H., Chatelard, P., Chailan, L., Hermsmeyer, St., Sanchez, V., Herranz, L. (2018) ″CESAM – Code for European severe accident management, EURATOM project on ASTEC improvement″, *Annals of Nuclear Energy*, Vol. 116, pp. 128-136

[7] Chatelard, P., Belon, S., Bosland, L, Carénini L., Coindreau O., Cousin F., Marchetto C., Nowack H., Piar L., Chailan L. (2016) ″Main modelling features of the ASTEC V2.1 major version″, *Annals of Nuclear Energy*, Vol. 93, pp.83-93

[8] Cranga, M., Fabianelli, R., Jacq, F., Barrachin, M., Duval, F. (2005) ″The MEDICIS code, a versatile tool for MCCI modelling″, Proc. of ICAPP'05, Seoul, Korea

[9] Nijhawan, S. (2014) ″CANDU 6 severe accident issues for Cernavoda″, CNCAN seminar, Bucharest, Romania

[10] Coindreau, O. (2017) ″ASTEC V2.1: Physical modelling of the ICARE module", Rep. no. PSN-RES/SAG/2016-00422 BDD-ST SAG-2016-310, IRSN, Cadarache, France, pp. 540

[11] Volchek, A., Zvonarev, Y., Schanz, G. (2004) ″Advanced treatment of zircaloy cladding high temperature oxidation in SA code calculations: Part II. Best-fitted parabolic correlations″, *Nuclear Eng. and Design*, Vol. 232, pp.85-96

[12] Petoukhov, S.M., Mathew P.M. (2006) ″Status of MAAP4-CANDU code development and simulations of severe core damage accidents for a generic CANDU 6 plant″, Techn. Meeting on Severe Accident and Accident Management, Tokyo, Japan

[13] Atomic Energy of Canada Limited (1979) ″4x600 MWe CANDU-PHW Nuclear Generating Station, Technical Description″, Vol. 4, AECL, Canada

[14] Cranga, M., Spindler, B., Dufour, E., Dimov, D., Atkhen, K., Foit, J., Garcia-Martin, M., Sevon, T., Schmidt, W., Spengler. C. (2010) ″Simulation of Corium Concrete Interaction in 2D Geometry″, *Progress in Nuclear Energy*, Vol. 52, pp.76-83

[15] Dufour, E., Spindler, B., Cranga, M., Dimov, D., Atkhen, K., Foit, J., Garcia-Martin, M., Sevon, T., Schmidt, W., Spengler, C. (2008) ″Simulation of corium concrete interaction in a 2D geometry: recent benchmarking activities on experiments and reactor cases″, European Review Meeting on Severe Accident Research (ERMSAR08), Nessebar, Bulgaria

[16] Cranga, M., Michel, B., Mun, C., Barrachin, M. (2010) ″Outcome of the available 2D MCCI experimental database for the reactor case in dry conditions″, MCCI-OECD seminar, Cadarache, France

[17] Cranga, M., Michel, B., Duval, F., Mun, C. (2007) ″Relative impact of MCCI modeling uncertainties on reactor basemat ablation kinetics″, MCCI-OECD seminar, Cadarache, France

[18] Cranga, M., Mun, C., Michel, B., Duval, F., Barrachin, M. (2008) ″Interpretation of real material 2D MCCI experiments in homogeneous oxidic pool with the ASTEC/MEDICIS code″, Proc. of. ICAPP'08, Anaheim, USA

[19] Bonnet, J.M. (2000) ″Thermal hydraulic phenomena in corium pools for ex-vessel situations: the BALI experiment″, Proc. of. Int. Conf. in Nuclear Engineering (ICONE8), Baltimore, USA